

Low Latency IoT/M2M Using Nano-Satellites

van 't Hof, Jos; Karunanithi, Visweswaran; Speretta, Stefano; Verhoeven, Chris; McCune, E.W.

Publication date

2019

Document Version

Final published version

Published in

70th International Astronautical Congress (IAC), Washington D.C., United States, 21-25 October 2019

Citation (APA)

van 't Hof, J., Karunanithi, V., Speretta, S., Verhoeven, C., & McCune, E. W. (2019). Low Latency IoT/M2M Using Nano-Satellites. In *70th International Astronautical Congress (IAC), Washington D.C., United States, 21-25 October 2019* (Vol. 2019-October). Article AC-19-B4.7.12 (Proceedings of the International Astronautical Congress, IAC). IAC.

Important note

To cite this publication, please use the final published version (if applicable).
Please check the document version above.

Copyright

Other than for strictly personal use, it is not permitted to download, forward or distribute the text or part of it, without the consent of the author(s) and/or copyright holder(s), unless the work is under an open content license such as Creative Commons.

Takedown policy

Please contact us and provide details if you believe this document breaches copyrights.
We will remove access to the work immediately and investigate your claim.

IAC-19-B4.7.12

Low Latency IoT/M2M Using Nano-Satellites

Jos van 't Hof^{a*}, Visweswaran Karunanithi^b, Stefano Speretta^c,
Dr. Chris Verhoeven^d, Prof. Earl W. McCune^e

^a Department of Microelectronics/Department of Space Engineering, Delft University of Technology (TU Delft), Mekelweg 5, 2628 CD Delft, The Netherlands, J.J.VantHof@student.tudelft.nl

^b Department of Microelectronics/Innovative Solutions in Space. BV, Delft University of Technology (TU Delft), Mekelweg 5, 2628 CD Delft, The Netherlands, V.Karunanithi-1@tudelft.nl

^c Department of Space Engineering, Delft University of Technology (TU Delft), Mekelweg 5, 2628 CD Delft, The Netherlands, S.Speretta@tudelft.nl

^d Department of Microelectronics, Delft University of Technology (TU Delft), Mekelweg 5, 2628 CD Delft, The Netherlands, C.J.M.Verhoeven@tudelft.nl

^e Department of Microelectronics, Delft University of Technology (TU Delft), Mekelweg 5, 2628 CD Delft, The Netherlands E.w.McCunejr-1@tudelft.nl

* Corresponding Author

Abstract

Nano-satellite IoT/M2M missions are gaining popularity in recent time. Various companies have launched their pilot missions last year in 2018 and all these companies intend to place a constellation in (V)LEO that can communicate with low power sensors on the ground (sometimes remote locations) and relay it back to the end-user who is monitoring these sensors. This paper discusses two possible architectures of using nano-satellites for low latency IoT/M2M, by presenting information such as, number of satellites needed, number of orbital planes needed and communication strategy. The first proposed architecture will comprise of a self-sustaining network of nano-satellites that communicate with low power, low data-rate sensors on the ground and relay the data to rest of the nano-satellites in the network using inter-satellite links, which is downlinked by a nano-satellite that is in the view of a ground station that is connected to IMT. The second proposed architecture will use nano-satellites to communicate with low power, low data-rate sensors on the ground and relay it to satellites that intend to provide internet from space (Mega-constellation). The internet constellations considered in this study for the second architecture are: Telesat's constellation, SpaceX's Starlink, OneWeb's constellation, Astrome's SpaceNet constellation and Audacy's constellation. Using both these architectures, it can be seen that the latency can be reduced considerably.

Keywords: IoT, latency, nano-satellite, inter-satellite link, (mega-)constellation

Acronyms/Abbreviations

DSA	Delay Sensitive Application
DTA	Delay Tolerant Application
FoV	Field of View
GEO	Geostationary Orbit
IMT	International Mobile Telecommunication
IOMT	Internet of Military Things
IoRT	Internet of Remote Things
IoT	Internet of Things
ISL	Inter-Satellite Link
LEO	Low Earth Orbit
M2M	Machine to Machine
MEO	Medium Earth Orbit
NGSO	Non Geo Stationary Orbit
RF	Radio Frequency
SSO	Sun Synchronous Orbits
UTCG	Universal Time Coordinated in Gregorian format
VLEO	Very Low Earth Orbit

1. Introduction

1.1 Motivation

Nano-satellite missions aimed at providing connectivity for Internet of Things (IoT)/Machine-to-Machine (M2M) applications are gaining popularity. Companies such as Hiber, Fleet, Lacuna Space and Kepler are planning to put constellations of nano-satellites into Low Earth Orbit (LEO) or Very Low Earth Orbit (VLEO) that can connect with sensors world-wide [1-4]. The nano-satellites in these missions collect data from remote locations on Earth that do not have other means of connectivity and forward it to ground stations connected to the internet.

With the capabilities of nano-satellites increasing the communication architectures for these satellites also increases in complexity. Nano-satellite technology exist that allows the nano-satellites to downlink their data at gigabit speeds at high frequencies where more bandwidth is available [5]. Some of the nano-satellite constellations

are planning to use Inter-Satellite Links (ISLs) to create a network in between the satellites of the constellation. For example the nano-satellites in the constellation of Kepler will be using Radio Frequency (RF) ISLs at Ka-band frequencies [4]. Also hardware for optical communication is being developed at this moment [6].

At the same time another revolution in satellite-based connectivity is going on with the rise of the Non-Geostationary Orbit (NGSO) satellite constellations that aim to provide global broadband connectivity from space. The networks created by the constellations of Telesat, SpaceX and OneWeb (also called “mega-constellations” because of their number of satellites) could achieve a high total system throughput [7]. This throughput is an order of magnitude higher than what can currently be achieved with the highest data rate communication systems for nano-satellites.

However, these constellations are focussed on providing broadband connectivity involving high data rates at high frequencies and require the user to have parabolic dishes of around half a meter or some equivalently phased array antenna system [8, 9]. These requirements are less appropriate for IoT/M2M applications. Where there is a focus on low power, low data rate and low frequency. An option could be to let the nano-satellites communicate with the IoT/M2M applications and relay the data through large NGSO satellite constellations.

This paper discusses two communication architectures for IoT/M2M nano-satellite missions. The first architecture considers a self-sustaining network of nano-satellites that communicate with low power, low data-rate sensors on the ground. After receiving the data, the nano-satellites will relay the data to rest of the nano-satellites in the constellation using ISLs. The data will be eventually downlinked by a nano-satellite that is in view of an International Mobile Telecommunication (IMT) connected ground station. In the second architecture the nano-satellites instead relay their data to a higher NGSO constellation that intends to provide global broadband connectivity from space.

1.2 Paper objectives

The main objective of this paper is to perform a first order comparison between two communication architectures for nano-satellites in IoT/M2M mission from a latency perspective; one architecture using a self-sustaining network of nano-satellites, the other using higher NGSO satellites to relay data. Later studies, for which this study forms the basis, will investigate the requirements for the RF communication systems in each of the architectures and estimate their total throughput. This paper will also introduce a purpose build NGSO data relay simulator that is used to find a first order estimation of the availability of a data relay between a nano-satellite and a higher orbit NGSO constellation.

1.3 Paper structure

This paper is structured as followed: Section 2 will give a description of the two IoT/M2M communication architectures, IoT/M2M use-cases and protocols and will discuss the NGSO satellite constellations that are considered to use as a data relay; Section 3 describes the models used to compute and compare the latency of the two communication architectures; Section 4 will present the results of the latency analysis of the two architectures. Section 5 will compare the two architectures; and Section 6 will present the conclusions.

2. IoT/M2M mission architecture overview

This section gives a description of the two proposed architectures, it will present some IoT/M2M applications and communication protocols and it will give a description of the NGSO constellations that were considered for the data relay architecture.

2.1 Description of architectures

In this work two architectures for nano-satellite IoT/M2M mission are considered; a self-sustaining constellation of nano-satellites and a constellation of nano-satellites that uses higher NGSO constellations to relay data.

Fig. 1 shows an illustration of the self-sustaining nano-satellite constellation architecture. In this architecture the nano-satellites in (V)LEO communicate with the low data-rate IoT/M2M users on the ground using common IoT/M2M communication standards. The constellation is self-sustaining because of the network the satellites create using ISLs. This self-sustaining network allows the satellites to relay the received data to the rest of the nano-satellites in the network. The data is eventually downlinked by a nano-satellite that is in view of a ground station connected to IMT.

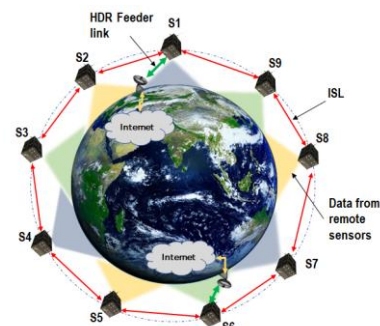


Fig. 1. Illustration of a self-sustaining nano-satellite IoT/M2M constellation [10].

Fig. 2 shows an illustration of the nano-satellites constellation that uses higher NGSO data relays. Like the first architecture the nano-satellites in (V)LEO also communicate with the IoT/M2M users on the ground. However, instead of having a network with ISLs the nano-satellites can individually relay the data through

NGSO constellations. In this architecture the nano-satellite constellation can take advantage of the large throughput that NGSO constellations offer. After relaying the data routing and downlinking the data is taken care of by the NGSO constellation.

The Velox-II satellite has already demonstrated this type of relay to a geostationary orbit (GEO) data relay satellite [11, 12]. In addition, the Commcube 1 satellite will attempt to communicate with the GlobalStar constellation [13].

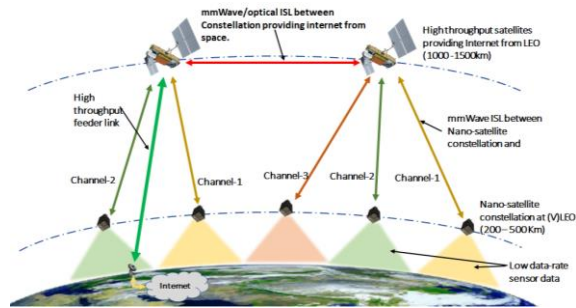


Fig. 2. Illustration of a nano-satellite IoT/M2M constellation using NGSO constellations to relay data [10].

2.2 Use cases and latency requirements

This section provides an overview of IoT/M2M use-cases based on literature in [14-18] and their latency requirements. The IoT applications can be broadly classified into delay tolerant applications (DTA) and delay sensitive applications (DSA). The DSA use-cases typically have a latency requirement in the order of few milliseconds to seconds [16]. These applications include smart homes applications, Internet of Military Things (IOMT), Internet of Remote Things (IORT) in smart grids. The DTA use-cases tolerate larger latency and can

be categorized as high and moderately high latency applications which are in the order of few minutes to hours.

The energy/smart grid use case is described in [16] with a detailed analysis on the latency requirements. With the advancements in automation of the power grids aspects such as timely communication of monitoring information, controlling and transmission of emergency alarms becomes crucial. The data traffic types for this use-case are; network monitoring (packets of 32 bytes), network alarms (packets of 60 bytes), control commands (packets of 60 bytes) and coordination traffic (packets of 1000 bytes). Among these types the network alarm packets have the lowest latency requirements, in the order of less than 1 second. Coordination traffic is less stringent with a latency requirement of 90 seconds. For use-cases such as geological disaster monitoring and weather forecasting, the latency requirement is moderate in the order of seconds and considered “Moderately low latency”. IoT through satellites can play a very crucial role in e-health care and elderly assistance especially in remote locations. The latency requirement for this use-case can be low when emergency alerts need to be sent from user terminal to an emergency room but may still be larger than 1 second. IoMT is another use-case where secure and reliable near real-time communication could be an significant advantage [18].

The DTA use-cases do not have a very stringent requirement on latency. One such use-case is logistics, transportation and asset tracking. The frequency of data collection from the user terminals for this use-case can be in the order of hours. The main advantage of using satellite based IoT for such an application is the larger coverage and access to remote locations for example oceans when tracking ships. Another use-case where satellites can play a key role is smart agriculture/farming.

Table 1 Overview of IoT/M2M use cases and their latency requirements.

	Service sector	Location	Devices	Requirement	Ref.
DSA	Energy/Smart grid	Power generation (distributed over large geographical areas), sub-stations, smart metering.	Solar panels, windmills, Distribution centers and substations, power meters	Near real-time	[16]
	Geologic disaster forecasting and weather monitoring	Disaster prone areas (earthquake, volcano), coastal areas, river beds, large forest covers.	Distributed electro-mechanical, Temperature monitoring.	Moderately low latency	[15]
	Healthcare and elderly assistance	Homes located in urban and remote locations, Hospitals, Elderly homes.	Electro-medical sensors	Moderately low latency	[14, 17]
	Internet of Military Things (IOMT)	Logistics, weapon support, environment monitoring, ISR and C2.	Radars, imaging sensors, Sonars, RFID	Near real-time	[18]
DTA	Logistics and transportation	Maritime, Aeronautical, Airports, harbors.	Vessels, cargo and passenger aircrafts, terrestrial communication infrastructure.	Moderately high latency	[14]
	Smart farming/agriculture	Large cattle farming areas spread into remote locations, Large agricultural areas	Cattle tracking and health monitoring, soil moisture monitoring.	High latency	
	Environment monitoring	Large forest areas, Mountains	Tracking wild animals and endangered species	High latency	[14]

In the case of agriculture, various types of sensors could be deployed over a large land area to monitor the health of the crop and moisture content to improve the yield. Similarly, in the case of farming, cattle tracking, and monitoring could be challenging when spread over very large area, in such cases satellite based IoT can help with the advantage of large coverage. Since this type “monitoring and tracking” type of data is not expected to change with-in a short period of time, the latency requirement for this application is assumed to be in the order of thrice to four times a day (6 to 8 hours). A similar use-case with a similar latency requirement is tracking wild and endangered species in large forest areas.

Table 2 summarizes the latency requirement classifications and their corresponding data type that is communicated through the user terminal. It can be inferred that emergency and protection related service information need low latency/near-real time requirements, controlling and monitoring needs moderately low latency, monitoring information from fast moving objects need moderately high latency and tracking information from slow moving objects can have high latency.

Table 2. Overview IoT/M2M communication protocols

	Data delivery duration	Data types
DSA	Near real time	< 1 s - Emergency services - Protection
	Moderately low latency	1 to 90 s - Controlling - Monitoring
DTA	Moderately high latency	< 1 h - Monitoring & tracking (fast moving objects)
	High latency	6 to 8 h - Monitoring & tracking (slow moving objects)

2.3 IoT/M2M communication standards

Looking at existing IoT standards is fundamental to better define the final constellation performances, both in terms of latency and throughput. First it is important to define which current IoT standard would lead to the best performances on a ground to space link. It is important to note that implementing an IoT network in space aims mainly at a global coverage and this could be complex given that most services operate on country-specific bands and sometimes protocols (mainly driven by pre-existing spectrum allocations).

Table 3. Overview IoT/M2M communication protocols

Protocol	Frequency	Bandwidth	Protocol Latency	Mode	Bitrate	Notes
LoRa(WAN)	433 MHz, 868 MHz, 915 MHz	125 kHz, 250 kHz, 500 kHz	0.1 – 3 s	Half-duplex	0.25 - 11 kbps	Demonstrated Ground to LEO with 125 kHz bandwidth
NB-IOT	617 – 2200 MHz	180 kHz	10 ms	Half-duplex	62 kbps	
Sigfox	868 MHz 902 MHz	600 Hz	330 ms	Half-duplex	600 bps	Closed standard, low power and narrow band
LTE-M		1.4 MHz	100 ms	Half-duplex	< 1 Mbps	LTE compatible, designed for cellular networks
Iridium Edge	1621 MHz	-	-	Half-duplex	2400 bps	Designed for space applications

As shown in Table 3, five main IoT standard have been analysed [19]: the most important characteristics for our analysis are the communication band, the data throughput, transmission latency (seen as the time required to transmit the smallest information unit) and eventual characteristics that would make the standard difficult to implement in a space-based receiver.

LoRa is a very popular standard for IoT devices employing a chirp spread spectrum modulation: this makes the signal quite insensitive to narrow-band interferers and provides high de-spreading gains, allowing a low-power implementation. LoRa is based on an open network definition, allowing independent suppliers to implement it. This also allowed the successful demonstration of space reception of ground nodes [20], making it one of the prominent choices for the constellation described in this paper.

SigFox [21], on the contrary, is based on a closed network infrastructure and, so far, saw no in-space demonstration. SigFox also shows a very narrow-band implementation that could suffer from interference when received from space (due to the much wider number of nodes that can be received from space).

NB-IoT and LTE-M [22] have been implemented to coexist with 4th generation cellular networks, making them very suited for high bandwidth applications (still with respect to small sensors) but hard to implement on a space receiver (mainly due to the modulation selection and the round-trip-time constraints, typical in cellular phones).

Iridium Edge requires a special mention as it is the only protocol designed for space applications but, being used already in a LEO constellation, would not fit the constellation being targeted in this article.

2.4 Overview of NSGO constellations

For the second architecture the NSGO constellations considered in this work are: Telesat’s LEO constellation, SpaceX’s Starlink LEO constellation, OneWeb’s LEO constellation, Astrome’s SpaceNet constellation and Audacy’s MEO relay constellation. Some of these NSGO constellations are considered “mega-constellations” due to their large number of satellites. Table 4 shows an overview of these NSGO constellations.

For analysing the latency of the data relay architecture of interest are the number of satellites, their orbital parameters and their fields of view (FoVs). In a later study that will focus on the design of the RF system on the nano-satellite the user frequency bands, user bandwidth and user beam types are of interest.

The next sections will shortly describe the properties of each of the NGSO constellations based on their FCC filings and published materials. An extensive discussion of the orbital configurations and beam patterns of Telesat's, OneWeb's and SpaceX's constellations can also be found in [7].

2.4.1 Telesat LEO constellation

In November 2016 Telesat Canada filed its first application for a LEO constellation of 117 satellites operating in Ku/Ka-band [23]. In March 2017 Telesat has requested approval for a separate LEO constellation operating in V-band [24].

This study considers Telesat's initial LEO constellation as defined in [23]. The 117 satellites in this constellation are placed in 11 orbital planes. Of these orbital planes six are circuit polar orbits at 1000 km, 99.5° inclination with each 12 satellites per plane and five are circular inclined orbits at 1200 km, 37.4° inclination with each 9 satellites per plane. Fig. 3 shows Telesat's LEO constellation inside the NGSO relay simulator. The figure also shows a nano-satellite in a 500 km polar orbit with an ISL to one of the Telesat satellites as reference.

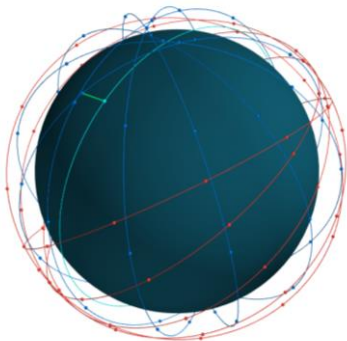


Fig. 3. Telesat LEO constellation inside the NGSO relay simulator together with a nano-satellite. The figure shows Telesat's polar orbits (blue) and inclined orbits (red), and the nano-satellite orbit (cyan) around Earth

Each of Telesat's satellites will serve users that can see the satellite down to an elevation angle of 10° [23]. This gives a FoV of $\pm 58.34^\circ$ for the 1000 km orbits and $\pm 55.43^\circ$ for the 1248 km orbits. Users will initiate communication with the satellite through the satellites fixed wide-area beam. After the initiation the satellite will provide the communication with the user with its shapeable and steerable user-beams of which there are at least 16 available on each satellite.

The user uplink band is 17.8 – 20.2 GHz (Ka-band) with a theoretical maximum bandwidth of 500 MHz. The user downlink band is 27.5 – 30 GHz with a theoretical maximum bandwidth of 850 MHz. The constellation uses optical ISLs that allows any two adjacent satellites to communicate regardless of their orbital planes. This allows a satellite to forward its data to a satellite that is in view of an internet connected ground station.

2.4.2 SpaceX Starlink LEO constellation

In November 2016 SpaceX filed its first application for a LEO constellation of 4425 satellites [25]. In March 2017 SpaceX has requested approval for a VLEO extension to this constellation with an additional 7518 satellites [26]. In November 2018 SpaceX requested to modify the altitude of the satellites in the lowest shell of satellites in the original constellation of 4425 satellites to 550 km [27] and change the number of planes and satellites per plane in this lower shell in later in August 2019 [28].

This study considers the LEO part of the constellation of SpaceX as defined in [28]. The 4409 satellites in this constellation are placed in five (spherical) orbital shells. The first shell at 550 km altitude has 72 planes at 53.0° inclination with each 22 satellites per plane. The second shell at 1110 km altitude has 32 planes at 53.8° inclination with each 50 satellites per plane. The third shell at 1130 km has 8 planes at 74.0° inclination with each 50 satellites per plane. The fourth shell at 1275 km has 5 planes at 81.0° inclination with each 75 satellites per plane. The fifth and final shell in the LEO constellation at 1325 km altitude has 6 planes at 70.0° inclination with each 75 satellites per plane. Fig. 4 shows SpaceX's LEO constellation inside the NGSO relay simulator. The figure also shows a nano-satellite in a 500 km polar orbit with an ISL to one of the SpaceX's satellites as reference.

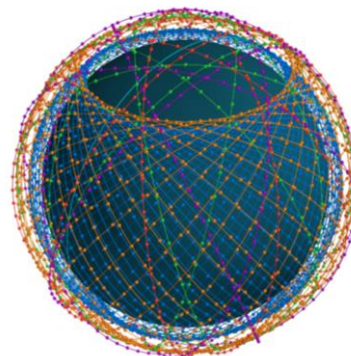


Fig. 4. SpaceX Starlink LEO constellation inside the NGSO relay simulator together with a nano-satellite. The figure shows Starlink's 550 km orbits (blue), 1100 km orbits (orange), 1130 km orbits (green) and 1325 km orbits (red), and the nano-satellite orbit (cyan) around Earth

After full deployment of the constellation each satellite will serve users that can see the satellite down to an elevation angle of 40° [25]. This gives an FoV of $\pm 44.85^\circ$ for the 550 km altitude satellites (also specified in [27]), $\pm 44.85^\circ$ for the 550 km altitude satellites, $\pm 40.72^\circ$ for the 1110 km altitude satellites, $\pm 40.59^\circ$ for the 1130 km altitude satellites, $\pm 39.67^\circ$ for the 1275 km altitude satellites and $\pm 39.67^\circ$ for the 1325 km altitude satellites. The SpaceX satellites use steerable and shapeable user beams of which there are at least 8 available on each satellite [25].

The user uplink band is 12.75 – 14.5 GHz with a theoretical maximum bandwidth of 500 MHz. The user downlink band is 27.5 – 30 GHz with a theoretical maximum bandwidth of 1 GHz. The SpaceX satellites will use optical inter-satellite links between the satellites in the constellation [25].

2.4.3 OneWeb LEO constellation

In April 2016 OneWeb filed its first application for a LEO constellation of 720 satellites [8]. In March 2017 OneWeb filed an application for a V-band extension to the constellation with 1280 satellites in MEO when fully deployed [29]. In March 2018 OneWeb requested to double the number of planes in the initial LEO constellation to 36 and the number of satellites per plane to 55 increasing the total amount of satellites to 1980 [30]. However in an December 2018 interview OneWeb’s founder said the company is scaling back the LEO constellation to around 600 satellites [31].

This study considers OneWeb’s initial LEO constellation of 720 satellites as defined in [28] because of the intent of the company to scale back the constellation. This constellation would have 18 polar orbital planes at an altitude of 1200 km and an inclination of 87.9° with 40 satellites per plane [28]. Fig. 5 shows OneWeb’s initial LEO constellation inside the NGSO relay simulator. The figure also shows a nano-satellite in a 500 km polar orbit with an ISL to one of the OneWeb’s satellites as reference.

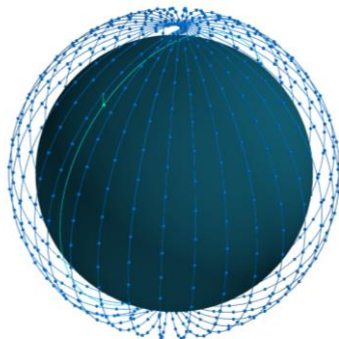


Fig. 5. OneWeb’s initial LEO constellation inside the NGSO relay simulator together with a nano-satellite. The figure shows OneWeb’s orbits (blue), and a nano-satellite orbit (cyan) around Earth.

Each of OneWeb’s satellites will serve users that can see the satellite down to an elevation angle of 55° [28]. This gives the 1200 km altitude satellites an FoV of $\pm 40.14^\circ$. The 16 user beams of OneWeb’s satellites are however fixed and elliptical, therefore a circular FoV is a simple approximation of the actual FoV.

The user uplink band is 14.0 – 14.5 GHz with a bandwidth of 125 MHz. The user downlink band is 10.7 – 12.7 GHz with a bandwidth of 250 MHz. The OneWeb satellites do not have an inter-satellite link and should therefore always be in line of sight of a ground station.

2.4.4 Astrome SpaceNet

Astrome’s has not filed FCC filings for its constellations yet. However they released two papers related to their constellation design in June 2019 [9] and July 2019 [32].

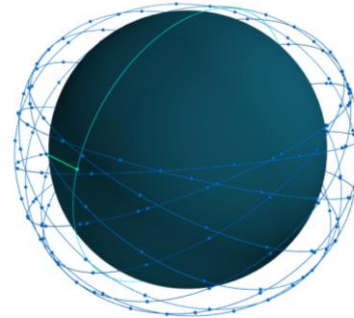


Fig. 6. Astrome SpaceNet constellation inside the NGSO relay simulator together with a nano-satellite. The figure shows SpaceNet’s orbits (blue), and a nano-satellite orbit (cyan) around Earth.

Astrome’s SpaceNet constellation is designed to provide coverage between $\pm 38^\circ$ latitude with 198 satellites from LEO [32]. The constellation has 11 orbital planes at an altitude of 1530 km and an inclination of 30° with each 18 satellites per plane [9]. Fig. 5 shows Astrome’s LEO constellation inside the NGSO relay simulator. The figure also shows a nano-satellite in a 500 km polar orbit with an ISL to one of the Astrome’s satellites as reference.

Each of Astrome’s satellites has a FoV of $\pm 37^\circ$ and uses digital beam forming to create multiple steerable spot beams [9].

The user uplink band is 81.0 – 86.0 GHz and the user downlink band is 71.0 – 76.0 GHz. Each satellite will have six RF inter-satellite links at 66.0 – 71.0 GHz to communicate with all neighbouring satellites [9].

2.4.5 Audacy MEO constellation

In December 2016 Audacy filed its application for a MEO constellation of 3 satellites [33]. Audacy’s constellation is the only one considered in this work that is not aimed at providing connectivity on earth from

space. Instead their MEO constellation is specifically designed as a data relay constellation for spacecraft in LEO.

The constellation consist of three satellites with at 13900 km at 25° inclination spaced 120° apart [33]. Fig. 7 shows Audacity's MEO constellation inside the NGSO relay simulator. The figure also shows a nano-satellite in a 500 km polar orbit with an ISL to one of the Audacity's satellites as reference.

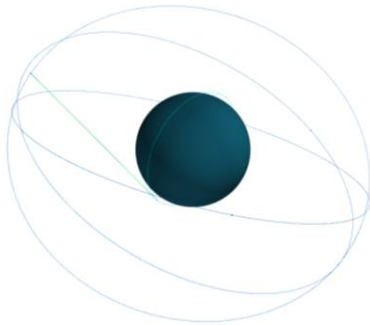


Fig. 7. Audacity's data relay MEO constellation inside the NGSO relay simulator together with a nano-satellite. The figure shows Audacity's orbits (blue), and a nano-satellite orbit (cyan) around Earth.

The relay satellites have a split FoV with an inner ring and an outer ring that are filled with spot beams. The inner ring is nadir pointing while the outer ring surrounds the earth up to 1500 km. The gaps in between the two beams of one relay satellite is filled with that of the other two [33]. Estimated from the figures in the FCC filing the FoV of the inner ring is approximately $\pm 16.55^\circ$ and the outer ring is from approximately 18.29° to 21.22° .

The relay satellites operate in K-band and V-band, the user uplink and downlink bands are 22.95 – 33.00 GHz with a maximal bandwidth of 600 MHz. The relay satellites also have dedicated spot beams for advanced users in a 10000 km field of view. The uplink and downlink bands are 22.55 – 32.8 GHz with a maximal bandwidth of 500 MHz for a single user. The relay satellites have RF inter-satellite links in the V-Band to forward data if one of the satellites cannot establish a connection to a ground station [33].

2.4.6 NGSO constellation discussion

The constellations of Telesat, SpaceX, OneWeb and Astrome all aim to provide broadband connectivity on the surface of the earth from space. The constellations of Telesat SpaceX and OneWeb aim to do so globally but with a vastly different number of satellites, orbital configurations and beam types as can be seen in Table 4. SpaceX having the largest number of satellites also has the overall highest number of satellites in line of sight from earth as was shown by [7].

These first four constellations are however optimized to provide ground coverage. Of the considered constellations for this work all except Audacity's aims to provide broadband connectivity on the surface of the earth from space. Fig. 8 shows a comparison of the FoVs of the satellites in each of the constellations projected on earth. Because of the limited FoVs of the satellites this means that at higher altitudes gaps in the coverage may exist.

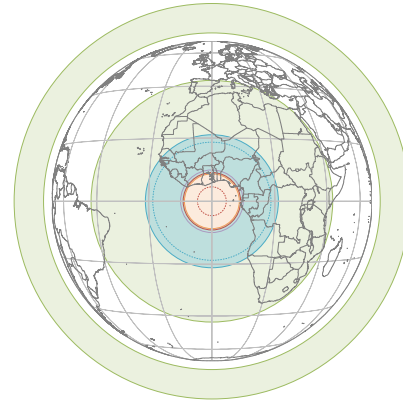


Fig. 8. Overlay of FoVs of NGSO satellites of Telesat LEO (blue), SpaceX Starlink (red), OneWeb LEO (orange), Astrome SpaceNet (purple) and Audacity (green). Dashed lines are the FoVs of the lowest altitude satellites in the constellation.

3. Methodology and model description

This section describes the methodology that was used to estimate the latency performance of IoT/M2M missions of the two communication architecture concepts. Fig. 9 and Fig. 10 show the models developed (grey-shaded rounded boxes) and the inputs (white boxes) and outputs (text) for the self-sustaining nano-satellite constellation architecture and the NGSO constellation relay architecture respectively. The dashed models are planned for future research.

Several elements contribute to the overall latency of the communication architecture. The latency considered in this paper is defined as the time between an IoT/M2M application having generated data and the time it took for the nano-satellite constellation to have forwarded this data to an IMT connected ground station.

The analysis of this paper is starts with a basic model for the nano-satellite constellation design that uses polar orbits. The number of satellites and number of planes in this constellation is chosen in such a way that the revisit time $t_{revisit}$, the time it takes for a location on earth to come in the FoV of the constellation is zero. In other words, it is optimized that every location on earth has can see at least one nano-satellite within a minimum elevation.

Table 4. Information of considered NGSO constellations for data relay

Constellation	Altitude	i	Number of:			User bands & (User bandwidth)		User beam Type	FoV
			Planes	Sats/Plane	Sats	Uplink	Downlink		
Telesat LEO	1000 km	99.5°	6	12	117	17.8 – 20.2 GHz (≤ 500 MHz)	27.5 – 30 GHz (≤ 850 MHz)	Steerable & shapeable spot beams	± 58.34° ± 55.43°
	1248 km	37.4°	5	9					
SpaceX Starlink LEO	550 km	53.0°	72	22	4409	12.75 – 14.5 GHz (≤ 500 MHz)	10.7 – 12.7 GHz (≤ 1 GHz)	Steerable & shapeable spot beams	± 44.85° ± 40.72° ± 40.59° ± 39.67° ± 39.36°
	1110 km	53.8°	32	50					
	1130 km	74.0°	8	50					
	1275 km	81.0°	5	75					
	1325 km	70.0°	6	75					
OneWeb LEO (2016)	1200 km	87.9°	18	40	720	10.7 – 12.7 GHz (250 MHz)	14.0 – 14.5 GHz (250 MHz)	Fixed elliptical beams	± 40.14°
Astrome Spacenet	1530 km	30.0°	11	18	198	81.0 – 86.0 GHz (< 500 MHz)	71.0 – 76.0 GHz (< 500 MHz)	Digital beam-forming spot beams	± 37.00°
Audacy	13900 km	25.0°	3	1	3	22.95 – 33.0 GHz (≤ 600 MHz)	22.95 – 33.0 GHz (≤ 600 MHz)	Spot beams	¹⁾ ±21.22°

1) There is a gap in the FoV of the relay satellites of Audacy between 16.55° and 18.29°

The user uplink model considers the time it takes to uplink the data, t_{uplink} , from the IoT/M2M application to the nano-satellite. This paper provides some examples for this latency using the protocols presented in section 2.3

For the first architecture, using the self-sustaining network between the nano-satellites, the rest of the latency is determined by the routing through the network, $t_{routing}$. This number is determined by the routing strategy in the network, the propagation and processing time from satellite to satellite and the time it takes to downlink the data $t_{prop,dl}$.

For the second architecture, using higher NGSO constellations for data relay, there is an additional element that causes latency. Namely the time it takes for the nano-satellite to come within FoV of the NGSO satellite. To find this delay time t_{delay} , the orbital dynamics between the nano-satellite and the higher NGSO constellation are simulated. From this simulation the availability of a data relay between the nano-satellite

and an NGSO satellite is extracted. The final delay for this architecture is determined by the routing speed of the NGSO constellation. For this latency advertised numbers of the NGSO constellations are taken.

The following sections describe each of the models in detail. Section 3.1 describes the orbit design of the nano-satellite constellations to provide the connectivity for the IoT/M2M applications. Section 0 describes the model used for the user uplink. For the first architecture, section 3.3 describes the routing strategy. For the second architecture, section 3.4 describes the orbital mechanics simulator, section 3.5 the relay availability model and section 3.6 the relay routing model. A summary of how the contributing delays add to the overall latency of the two architectures is provided in section 3.6.

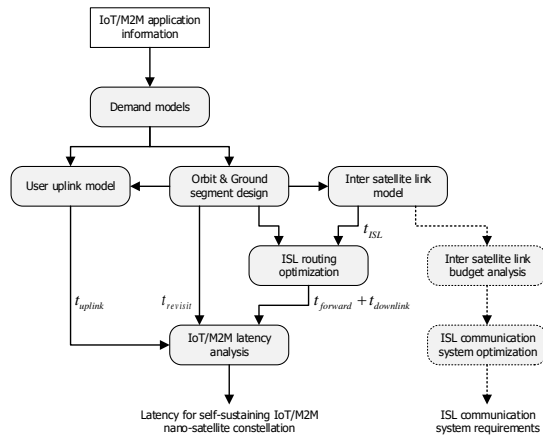


Fig. 9. Block diagram of the methodology employed to estimate IoT/M2M missions using the self-sustaining constellation of nano-satellites communication architecture

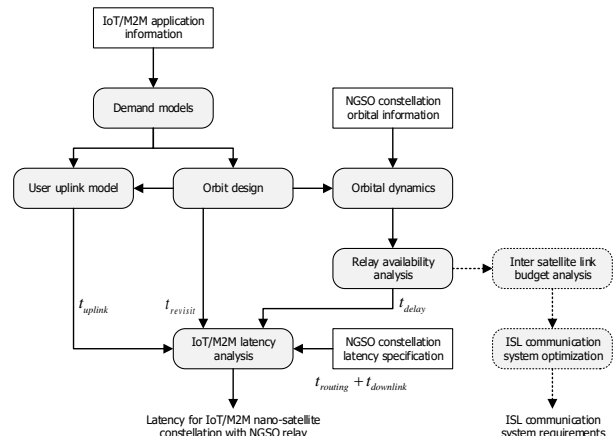


Fig. 10. Block diagram of the methodology employed to estimate IoT/M2M missions using a NGSO constellation relay concept.

3.1 Orbit design

The purpose of this paper is not to design the most optimal constellation for a specific use-case or cater to a specific region on Earth. Therefore, a simple constellation that can provide continuous global coverage using satellites in polar orbits is considered.

The purpose of this calculation is to find out the various possibilities in number of satellites needed per orbital plane and number of orbital planes for various combination of minimum elevation angle E_l and constellation altitude. All the calculations are done for single satellite coverage, when for a given E_l there is at least one satellite always visible.

The total number of satellites N needed for continuous global coverage in a polar orbit depends on the altitude of the constellation H and the coverage angle of the payload on the satellite. The half power beam-width of payload coverage is given by α . The corresponding half power earth centred cone is given by ψ . The total number of satellites is given by $N = n * m$, where n is the number of orbital planes and m is the number of satellites per orbital plane. To calculate the total number of satellites the needed for continuous global coverage with at-least one satellite in coverage, N must satisfy the following relation [34]:

$$N \cong \frac{4 * \cos(\lambda)}{1 - \cos(\psi)} \quad (1)$$

where:

$$\psi = \arccos\left(\frac{R_e}{R_e + H} * \cos(E_l)\right) - E_l \quad (2)$$

where λ is the coverage latitude. For global coverage λ is 0 degrees. In order to determine the number of satellites needed per orbital plane (m) and the number of orbital planes (n), based on [34] the relation between m and n must satisfy:

$$1.3n < m * \cos(\lambda) < 2.2n \quad (3)$$

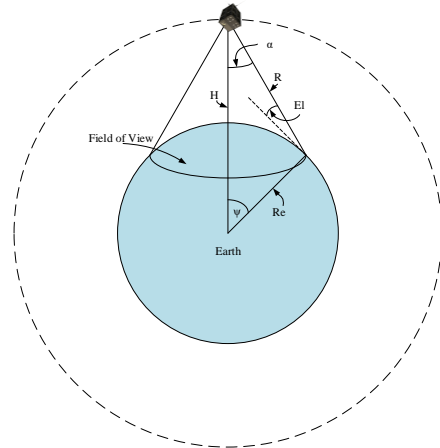


Fig. 11. Diagram of parameter definitions.

Based on the above equations, a plot of the number of satellites needed to form a constellation that can provide continuous global coverage is shown in the left graph of Fig. 12. In order to determine m and n using Equ. (3), m is chosen as $2n$ and the different combinations are shown in the middle graph of Fig. 12. Another parameter that is important with respect to the payload design is the half beam-width angle of the FoV α . The right graph of Fig. 12 shows the relation between α , H and E_l .

All these calculations correspond to a single satellite coverage, for three satellites coverage (at-least three satellites are within the coverage of a user terminal) the total number of satellites is given by:

$$N \cong \frac{11 * \cos(\lambda)}{1 - \cos(\psi)} \quad (4)$$

which must satisfy:

$$1.4n < m * \cos(\lambda) < 2.4n \quad (5)$$

In applications such as IoMT where reliability of a link between user-terminal and satellite is important multi-satellite coverage is preferred, which would result into a larger number of satellites.

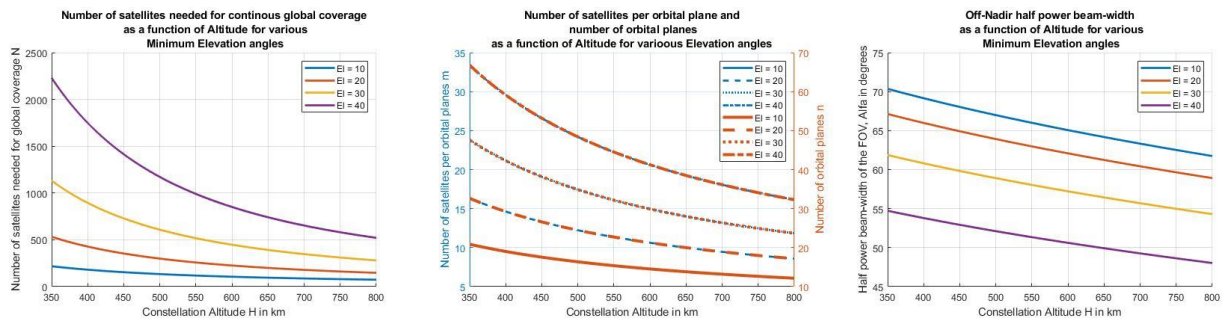


Fig. 12. Graphs showing properties of nano-satellite constellation for different altitudes

3.2 User uplink model

For this paper the user uplink model is kept simple. Three elements contribute to the t_{uplink} time; the time it takes to transfer a packet $t_{transfer}$, the set-up and overhead latency added by the protocol $t_{protocol}$ and the propagation delay from the ground to the nano-satellite $t_{prop,ul}$. This gives the following equation:

$$t_{uplink} = t_{protocol} + t_{transfer} + t_{prop,ul} \quad (6)$$

The protocol and transfer speeds for several packet sizes are shown in Fig. 13. For the propagation delay the slant range is calculated for different minimum elevation angles. The propagation delay is therefore:

$$t_{prop,ul} = \frac{d_{slant}}{c} \quad (7)$$

Fig. 14 shows the slant ranges at several elevation angles for different nano-satellite altitudes. Also plotted is the propagation delay assuming propagation with the speed of light. As can be seen the propagation delay is in the order of a few milliseconds. Comparing this to Fig. 13 the propagation delay quickly gets two orders of magnitude smaller than the protocol and transfer time. It is therefore expected that the larger contributors to the latency will be the protocol latency and the latency of the nano-satellite network, either self-sustaining or using NGSO relays.

3.3 Self-sustaining network routing

For the self-sustaining network of nano-satellites the $t_{routing}$ duration is defined as:

$$t_{routing} = \gamma \frac{N_s}{N_G} (t_{ISL} + t_{processing}) + t_{prop,dl} \quad (8)$$

In Equ. (8) the t_{ISL} duration is the time it takes for a single nano-satellite to forward its data to a neighbouring satellite in the same plane over the ISL. The $t_{processing}$ duration is the time required for on board processing on the nano-satellite for each ISL transmission and is based on [16] to be 3 ms. The total routing time depends on the number of nano-satellites in the chain N_s and the number of ground stations that have line of sight with the chain of nano-satellites N_G . It is assumed that at-least one satellite in any orbital plane can be seen by a ground station, this is possible if the ground stations are located near the poles and $N_G = 1$. The influence of the routing strategy is defined by the factor γ . For a bi-directional routing $\gamma=1/2$, for uni-directional routing $\gamma=1$. This work only considers ISL within an orbital plane and not between orbital planes. The $t_{downlink}$ for a self-sustaining architecture is considered for a worst-case scenario i.e., when the satellite is at its lowest elevation limit of 10 degrees, this corresponds to the longest propagation delay.

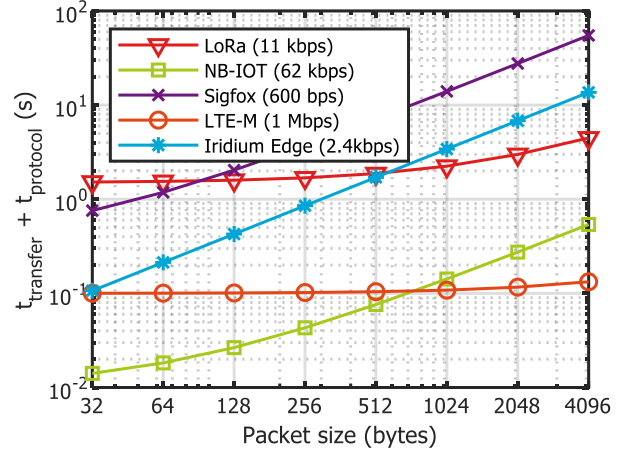


Fig. 13. Transfer speeds for different IoT protocols

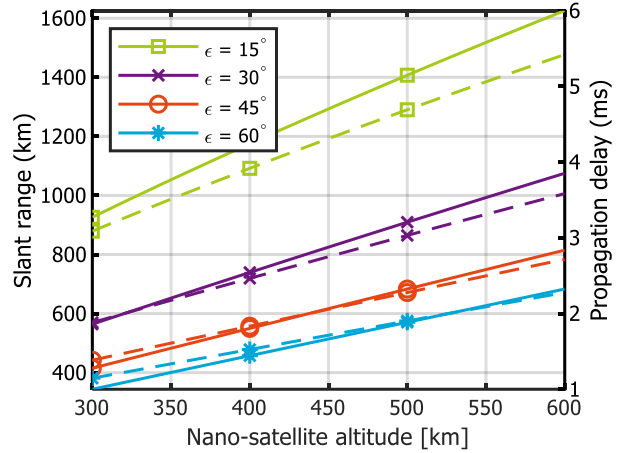


Fig. 14. Slant range (solid, left axis) and propagation delay (dashed, right axis)

3.4 Relay orbital dynamics

A purpose build tool was made to simulate the availability of the NGSO constellation data relay. The NGSO relay simulator is made in Python using the Poliastro Python package [35] for astrodynamics computation and the Mayavi library [36] for visualisation. The simulator is optimized for simulating a large amount of satellites simultaneously to find the lines of sight and pass durations while maintaining a reasonable accuracy. It uses two-body propagation and the Markley algorithm of solving Keplers equation [37].

The orbital mechanics of the simulator was validated by comparing a simple scenario in the free version of Analytical Graphics Incorporated Systems Toolkit® 11 using its two body propagator. Fig. 15 shows a side by side comparison of the simple scenario inside the two simulators. This scenario contains two satellites in circular orbits around Earth having orbital elements as defined in Table 5.

To compare the two simulators the (inter-satellite) pass duration (the time in which there was a line of sight between the two satellites) between the two satellites are analysed. The higher orbit satellite has a constrained

nadir pointing field of view that is varied in each of the cases. The lower orbit satellite has an unconstrained field of view. The analysis period is two hours starting at 1 September 2019 10:00:00.000 UTCG and the step size was set to 1 second.

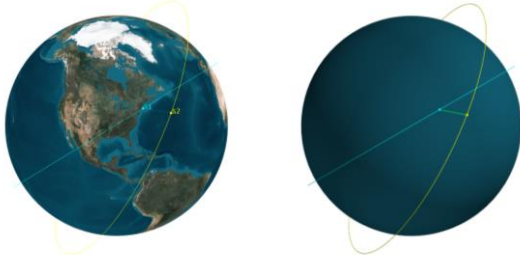


Fig. 15. Side by side comparison of a simple scenario with AGI's Systems Toolkit® 11 (left) and the purpose build simulator (right)

Table 6 shows the pass durations of the first pass encountered in the scenario. The pass duration found in the NGSO relay simulator corresponds to that in STK for all the cases. However, the adaptive step size computation in STK results to a much greater accuracy than is achieved with the fixed 1 second step size of the NGSO relay simulator.

Table 5. Orbital elements of the two satellites in the validation scenario

	Satellite 1	Satellite 2
$h_a(km)$	500	1500
e	1	1
$i(deg)$	45	60
$\Omega(deg)$	0	45
$u(deg)$	15	0
Epoch	J2000	J2000

Table 6. Contact durations of the first pass of the two satellites in the validation scenario

FOV	STK Simulator	NGSO relay simulator
$\pm 60^\circ$	1218.986 s	1218 s
$\pm 45^\circ$	463.702 s	462 s
$\pm 30^\circ$	246.317 s	246 s
$\pm 15^\circ$	100.317 s	99 s

For this paper a step size of 1 second is considered acceptable and accurate enough. With this step size the NGSO relay simulator can find the pass durations with an accuracy of $\pm 2s$. The minimum duration for a usable inter-satellite pass will be determined by the overhead in setup and connection time of the communication protocol used by the NGSO constellations. This number is unknown for the considered NGSO constellations however it is assumed that it will be in the order of seconds and not milliseconds. Without knowing the exact duration of the setup times, simulating with a smaller step sizes is not considered useful at this time.

3.5 Relay availability model

After the nano-satellite received the data from the IoT/M2M user it needs to wait until it gets in FoV of the higher orbit NGSO satellite to be able to forward this data. This duration is a contributor to the latency of the architecture that depends on the relative motion of the nano-satellite and the NGSO satellites. The Telesat, SpaceX, OneWeb and Astrome constellations are optimized for coverage on ground in their orbits, FoVs and (steerable) user beams. Therefore, the coverage in (V)LEO could be significantly lower for these constellations.

The NGSO relay simulator extracts the (inter-satellite) pass information while simulating the orbital dynamics. This information contains the positions of the two nodes during the pass, the start and stop time of the pass and its total duration. Based on this information the gap duration, the time in between two passes, can also be calculated. This gap duration, or more specifically its distribution, will contribute as a delay to the overall latency of this architecture.

The inter-satellite passes are simulated between a nano-satellite in a 500 km polar orbit and each of the NGSO constellations. Table 5 shows the orbital elements of this nano-satellite. It is assumed that the distributions of the passes are similar among the rest of the nano-satellites inside the IoT/M2M constellation. It is assumed that once the nano-satellite enters the FoV of the NGSO constellation satellite it can relay its data. The exact location of the spotbeams are therefore not considered. It could however be that not the entire FoV of the NGSO constellation satellite is covered by the spotbeams especially when the satellite uses shape able and or steerable spot beams.

Table 7. Orbital parameters of the single nano-satellite in polar orbit that is used as a reference for the IoT/M2M nano-satellite constellation.

	Nano-satellite orbital parameters
ha	500 km
e	1
i	90°
Ω	$0^\circ, 45^\circ, 90^\circ$ or 135°
v	0°
T	5677 s
Epoch	J2000

The NGSO relay simulator does not take any perturbations into account. Therefore, the effect of a perturbation such as the J2 perturbation that causes the right ascension Ω to over time at a constant rate is not modelled. This effect is also used to create Sun Synchronous Orbits (SSO) such as the ones used for the Kepler IoT constellation [4]. To compensate for this inaccuracy of the simulator the cases are repeated for varying values of the right ascension Ω .

3.6 Relay routing model

Round trip time numbers reported by the NGSO constellation companies or other studies are used to estimate the latency caused by routing through their satellite networks and downlinking the data to a ground station. Table 8 shows an overview of the latencies of the satellite networks. The analysis in [38] is by far the most realistic in as it takes into account the routing between the satellites when connecting two different places on earth. Whereas the other numbers only take the round-trip time from earth to the satellite and back.

Table 8. Round trip time numbers for the considered NGSO constellations

Constellation	Round trip time	Ref.
Telesat LEO	18 - 40 ms	[39]
SpaceX Starlink	50 - 75 ms	[38]
OneWeb LEO	32 ms	[40]
Astrome SpaceNet	10 ms	[32]
Audacy	< 1000 ms	[33]

3.7 Overall architecture latency

The overall latency of the architectures can be defined as followed:

$$t_{overall} = t_{revisit} + t_{uplink} + t_{delay} + t_{routing} \quad (1)$$

In Equ. (1) the $t_{revisit}$ duration is defined as the time it takes for an IoT/M2M constellation nano-satellite to come within view of the IoT/M2M user. As shown in section 3.1 this number can be reduced to zero if the nano-satellite constellation uses enough satellites in polar orbits. The t_{uplink} duration is defined as the total time it takes for an IoT/M2M user to uplink its data to the nano-satellite. Section 3.2 showed that this number is mainly dependent on the data rate of the link and the protocol latency and not on the propagation delay. The t_{delay} duration is the time it takes before the nano-satellite can forward the data through the network. For the self-sustaining network this number is zero if the ISLs are always on. For the NGSO constellation data relay this duration is the time it takes for the nano-satellite to come within the field of a NGSO satellite. Finally, the $t_{routing}$ is the rest of the time it takes for the data to travel through the network to an internet connected ground station. For the self-sustaining network of nano-satellites this number depends on the altitude of the constellation and the number of satellites as explained in section 3.3. For the NGSO constellation data relay the latency reported by the constellations were taken as explained in section 3.6.

4. Results

This section will present the results for the latency analysis of the architecture using the self-staining network of nano-satellites and the architecture that uses higher NGSO constellations to relay data.

4.1 Self-sustaining network

Based on the formulas discussed in section 3.1 to 3.3 the routing time $t_{routing}$ is calculated for the self-sustaining network of nano-satellites. This data is tabulated in Table 9.

Table 9. Routing delay for self-sustaining network of nano-satellites

El	H [km]	$t_{prop,up}$ [ms]	N	m	n	t_{ISL} [ms]	$\gamma N_s N_G^{-1} t_{hop}$ [ms]	t_{prop} [ms]	$t_{routing}$ [ms]
10°	350	4.35	218	21	10	6.73	101.49	4.35	105.83
	400	4.80	181	19	10	7.43	99.18	4.80	103.98
	450	5.23	154	18	9	8.11	97.45	5.23	102.68
	500	5.65	134	16	8	8.75	96.12	5.65	101.77
	550	6.05	118	15	8	9.38	95.10	6.05	101.15
20°	350	2.92	533	33	16	4.31	119.31	4.35	123.66
	400	3.28	428	29	15	4.84	114.71	4.80	119.51
	450	3.63	354	27	13	5.37	111.23	5.23	116.46
	500	3.98	299	24	12	5.87	108.52	5.65	114.17
	550	4.31	258	23	11	6.37	106.38	6.05	112.43
30°	350	2.17	1132	48	24	2.96	141.78	4.35	146.13
	400	2.46	894	42	21	3.35	134.36	4.80	139.15
	450	2.75	729	38	19	3.74	128.68	5.23	133.92
	500	3.03	608	35	17	4.13	124.24	5.65	129.89
	550	3.31	517	32	16	4.50	120.68	6.05	126.74

The switching/processing delay considered in the calculations is 3 mS, this is based on the assumption made in [16], this delay is protocol and data rate dependent and can vary for a different application. The calculations show that $t_{routing}$ delay can vary between 100 mS to 150 mS for different altitudes H and El considered.

4.2 NGSO data relay

Using the NGSO relay simulator the relay availability for a nano-satellite in a 500 km polar orbit to each of the NGSO constellations was analysed. For each of the constellations four different cases are simulated varying the right ascension Ω of the nano-satellite to compensate for perturbation effects not being taken into account in the simulator. All cases were simulated over 7 days starting at 1 September 2019 10:00:00.000 UTCG.

Fig. 16 and Fig. 17 show histograms of the pass and gap durations respectively for each of the five constellations. The histograms for the pass durations show each individual pass with a NGSO satellite. It is possible that at a particular moment the nano-satellite is able to communicate with multiple satellites in the NGSO constellation. The histograms for the gap durations are created by computing the time in which the nano-satellite was not in the FoV of any of the NGSO satellites in the constellation.

All histograms are fitted with a normal distribution to indicate the mean and variation of the pass and gap durations. As can be seen in Table 10 these do not vary significantly between the different cases for the right ascension Ω of the nano-satellite, except for the scenario of a relay to OneWeb's LEO constellation. The polar orbits of OneWeb make the pass and gap durations strongly dependent on whether or not the orbital plane of the nano-satellite lines up with one of the polar orbits in the constellation. In the right ascension $\Omega = 0^\circ$ case the plane lined up and more than double the number of passes are registered and the average gap duration decreased. However, the additional passes are of short duration and therefore lower the mean of the overall distribution.

The pass duration with the constellation of Astrome has the lowest variation. This is because the constellation has only set of orbits providing coverage between $\pm 38^\circ$ latitude. This also results into the gap distribution having two peaks. One with a long duration for the part in which the nano-satellite is traveling beyond $\pm 38^\circ$ latitude and one with a short for the part in which the nano-satellite is traveling within the $\pm 38^\circ$ latitude and passing between the satellites.

Even though the Audacity MEO constellation is designed for coverage in LEO the simulations show that the coverage is not continuous. These gaps are caused due to the line of sight intersecting the surface of the earth. At higher orbits it is possible that the coverage is continuously provided by the three satellites.

Table 10. Tabulated results of NGSO relay availability analysis

Ω	N_{passes}	μ_{pass}	σ_{pass}	N_{gaps}	μ_{gap}	σ_{gap}
<i>Telesat LEO</i>						
0°	1155	132 s	132 s	902	526 s	492 s
45°	837	162 s	98 s	710	668 s	480 s
90°	801	180 s	129 s	627	770 s	530 s
135°	948	148 s	112 s	770	612 s	527 s
<i>SpaceX Starlink LEO</i>						
0°	36574	132 s	145 s	1649	26 s	32 s
45°	38692	116 s	85 s	1133	24 s	28 s
90°	36343	119 s	91 s	1351	29 s	40 s
135°	36020	125 s	116 s	1238	25 s	31 s
<i>OneWeb LEO</i>						
0°	14996	158 s	272 s	2087	72 s	169 s
45°	6826	345 s	359 s	226	266 s	196 s
90°	6046	381 s	382 s	235	345 s	316 s
135°	7007	331 s	372 s	238	259 s	214 s
<i>Astrome SpaceNet</i>						
0°	2915	187 s	66 s	725	518 s	736 s
45°	2930	185 s	64 s	741	504 s	735 s
90°	2961	182 s	62 s	611	605 s	778 s
135°	3027	179 s	63 s	702	532 s	753 s
<i>Audacity</i>						
0°	331	1251 s	981 s	331	215 s	176 s
45°	757	1180 s	643 s	325	225 s	186 s
90°	705	1280 s	997 s	356	184 s	112 s
135°	676	1326 s	1096 s	328	206 s	138 s

Fig. 18 shows just the normalized distributions of the pass durations respectively. A relay with the Audacity constellation provides the longest pass durations, on average about 20 minutes.

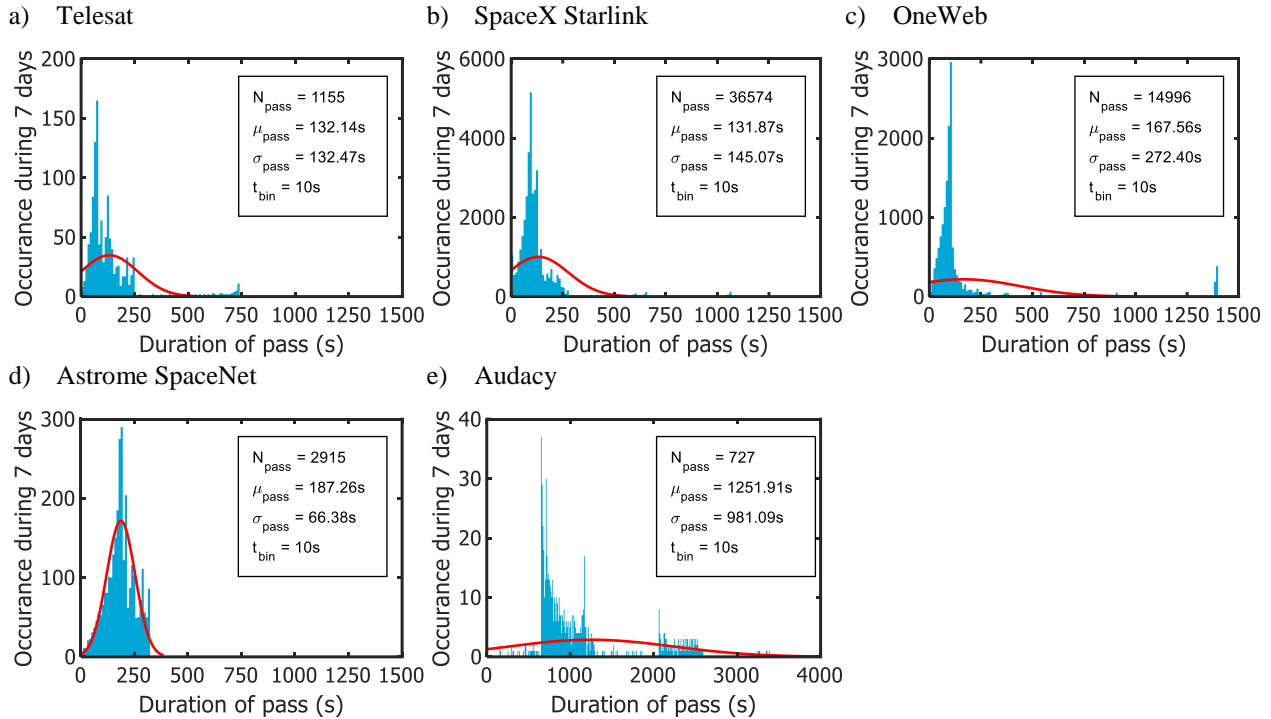


Fig. 16. Distributions of pass durations for a relay with a) Telesat LEO constellation, b) SpaceX Starlink constellation, c) OneWeb LEO constellation, d) Astrome SpaceNet constellation and e) Audacity constellation. *Note: the duration range for Audacity's histogram is larger than the other*

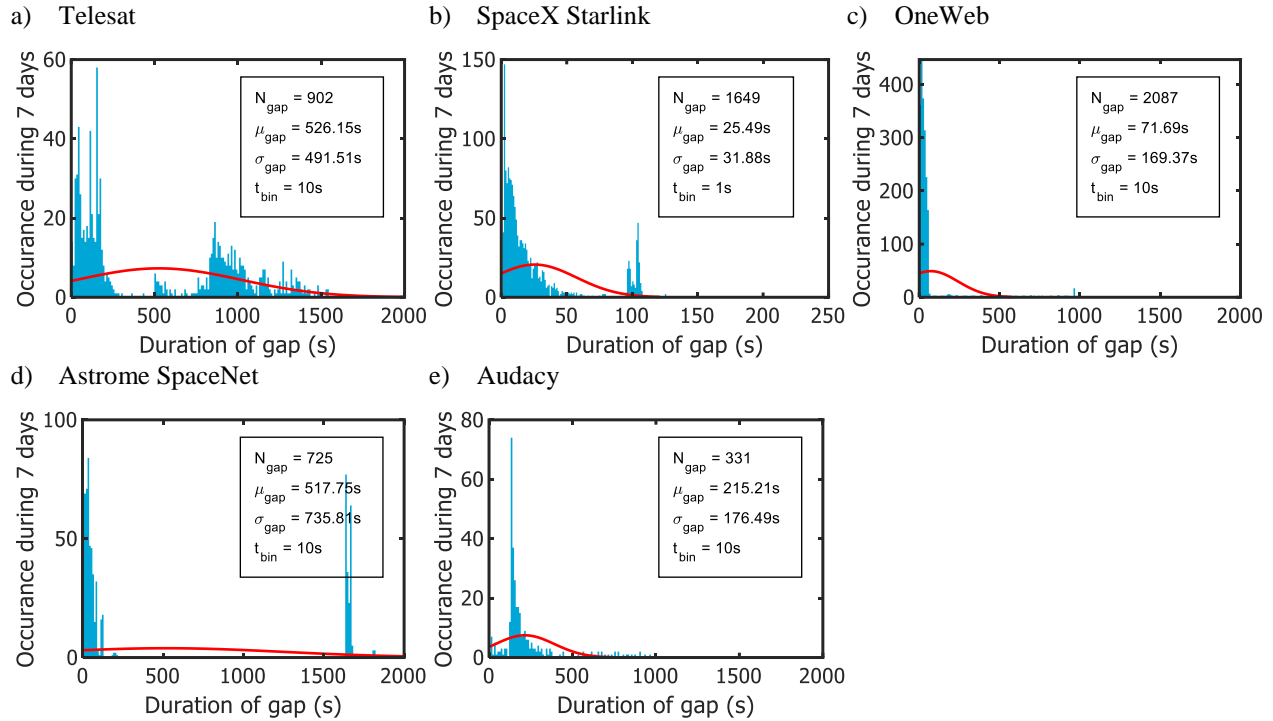


Fig. 17. Distributions of gap durations for a relay with a) Telesat LEO constellation, b) SpaceX Starlink constellation, c) OneWeb LEO constellation, d) Astrome SpaceNet constellation and e) Audacy constellation. *Note: the duration range for SpaceX's histogram is smaller than the others.*

The disadvantage is however the longer inter-satellite distance which requires a higher transmission power. The other constellations all provide a pass duration on average of about 2 to 4 minutes with SpaceX and Astrome having the lowest variance. It should be noted that the OneWeb constellation provides on average in this configuration 3 minutes of contact time, however as can be seen Fig. 16-c there are also significantly longer pass durations of about 20 minutes when the planes align and the nano-satellite can catch up with a satellite of OneWeb.

Fig. 19 shows just the normalized distributions of the gap durations. A relay with SpaceX would provide the lowest gap durations and therefore also the lowest average latency caused by the nano-satellite having to wait to come in view of the higher orbit NGSO satellite. OneWeb provides the second lowest gap duration on average and Audacy the third, caused by the line of sight intersecting the surface of the earth. Telesat and Astrome provide the longest gap duration on average due to the orbits being spaced out, in the case of Telesat, or concentrated around one region of the earth, in the case of Astrome.

A different metric to evaluate the latency of the NGSO data relay concept is to look at the total gap time over the whole simulation period.

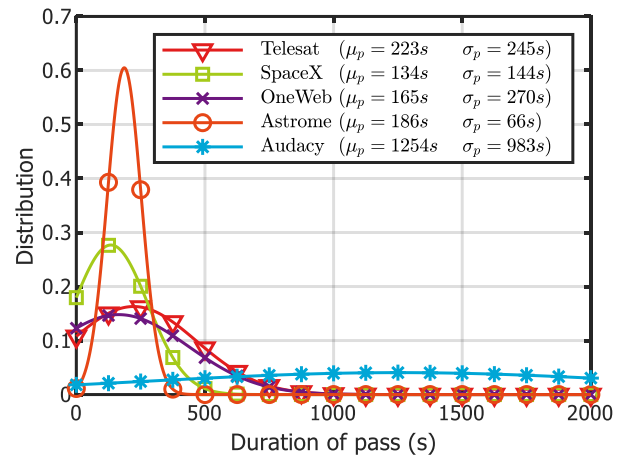


Fig. 18. Normalize pass distributions for a nano-satellite (500 km, $i = 90^\circ$, $\Omega = 0^\circ$) to higher orbit NGSO constellations.

Fig. 20 shows the total time the satellite is in darkness; the time where there is no relay available. Similar conclusions can be taken as to when just looking at the gap distributions. SpaceX and Audacy provide the most coverage, and Telesat and Astrome the least.

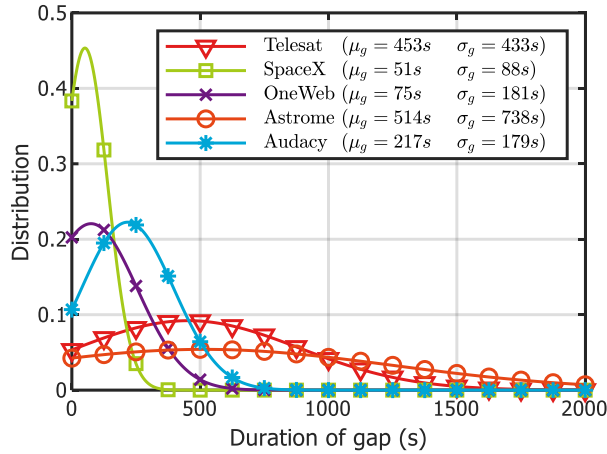


Fig. 19. Normalized gap distributions for a nano-satellite (500 km, $i = 90^\circ$, $\Omega = 0^\circ$) to higher orbit NGSO constellations.

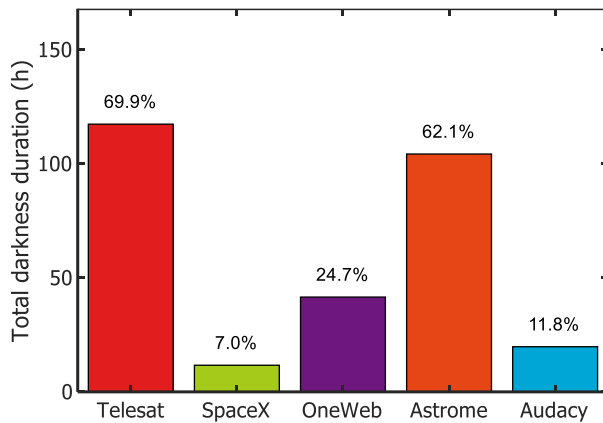


Fig. 20. Total darkness duration for a nano-satellite (500 km, $i = 90^\circ$, $\Omega = 0^\circ$) relay to higher orbit NGSO constellations during a 7-day period.

5. Discussion

Fig. 21 shows how each of the durations add up to the overall architecture latency in an example worse-case scenario. In this scenario a packet of 1024 bytes is uplinked to the nano-satellite using the LoRa protocol with a 3 second protocol latency. This results into an uplink latency of about 4 seconds. For the self-sustaining network of nano-satellites the constellation is selected to be at 500 km altitude with a user minimum elevation angle of 10° . This results into a routing latency of about 102 ms. For the architecture using the NGSO data relays the average gap duration and average routing delay is taken as the worse-case number.

For the self-sustaining network of nano-satellites the biggest contributor is the time to uplink the data to the satellite. Because the network from ISLs is always on the data can be immediately routed further. There is a disadvantage however with having a network of ISL that

is always turned on. In this case the duty cycle of the communication system is much higher than what is common for a nano-satellite. This requires a higher power budget on the satellite to be dedicated to maintaining these ISLs.

For the NGSO constellation data relay architecture the biggest contributor is the gap duration. Depending on when the data arrives at the nano-satellite there is a chance it can immediately relay this data, with a probability varying by the used relay constellation as seen in Fig. 20, or it has to wait up till several minutes before the relay becomes available, as shown in Fig. 19.

In the NGSO constellation data relay architecture the actual latency will therefore depend on at which point in the orbit of the nano-satellite the IoT/M2M data is received. Then at that moment the position of the nano-satellite with respect to the NGSO constellation should be considered. A possible analysis could be done on the average latency for an IoT/M2M application using this architecture depending on the latitude of its position.

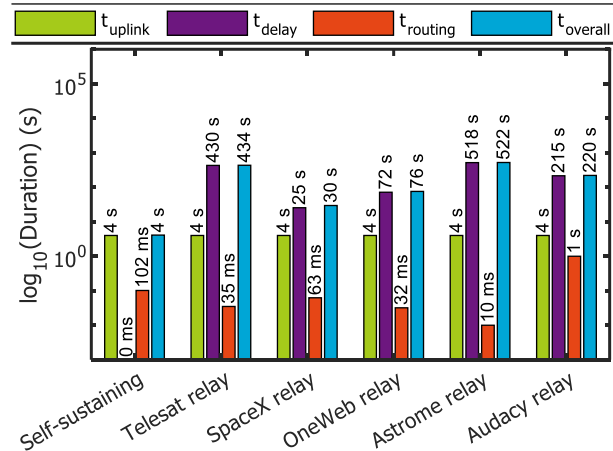


Fig. 21. Main contributing elements to overall latency in the architectures. For the relay architectures the mean gap duration and mean routing latencies are shown.

Some additional assumptions were taken for this architecture that might influence actual latency. First, the setup time required to setup the nano-satellite to NGSO constellation data relay could be in the order of seconds. Therefore, some of the inter-satellite passes can be immediately discarded because there is too little time to setup the link and start communicating. Second, the whole FoV of the NGSO constellation satellites might not be continuously filled with spotbeams and the spotbeams might be moving around. This could further reduce the effective communication time. In addition, frequency reuse schemes are used from spotbeam to spotbeam which depending on the protocol used might introduce some overhead in handovers. Finally, there were no limitations put on the communication system of the nano-satellite. The performance of this architecture will eventually come down to the capabilities of the

communication hardware on the nano-satellite. If the hardware on the nano-satellite can work in a wide FoV and can handle fast switching between spotbeams it can utilize most of the inter-satellite passes. Exploring the technical capabilities of the nano-satellite hardware is part of the roadmap of the authors of this paper.

6. Conclusions

In this paper two communication architectures for IoT/M2M nano-satellite missions are presented. The first architecture uses a self-sustaining network of nano-satellites. In this architecture the achievable latency can be in the order of seconds depending on the data rate of the IoT/M2M protocol. The latency through the network alone is always in the order of hundred milliseconds if the ISLs are kept turned on. For the communication system of this architecture this means a high duty cycle is required for a low latency. The second architecture uses planned NGSO constellations for data relay. A first order analysis showed that this architecture could achieve a latency down to several minutes which would be low enough for some IoT/M2M applications. The capabilities of the communication system of the nano-satellite to communicate in short inter-satellite pass durations will primarily determine the performance of this architecture.

Acknowledgements

The authors of this paper would like to thank Analytical Graphics Incorporated for providing a license for STK Free.

References

- [1] Hiber. (2019). www.hiber.global [Online]. Available: <https://hiber.global>.
- [2] Fleet. (2019). Fleet [Online]. Available: <https://www.fleet.space/>.
- [3] Lacuna Space. (2019). Lacuna Space [Online]. Available: <https://www.lacuna.space/>.
- [4] Kepler Communications Inc. (2016). Application for Fixed Satellite Service by Kepler Communications Inc. [SAT-PDR-20161115-00114] [Online]. Available: <https://fcc.report/IBFS/SAT-PDR-20161115-00114>.
- [5] K. Devaraj et al., "Planet High Speed Radio: Crossing Gbps from a 3U CubeSat," 2019.
- [6] R. Welle et al., "A CubeSat-Based Optical Communication Network for Low Earth Orbit," 2017.
- [7] I. del Portillo, B. G. Cameron, and E. F. Crawley, "A technical comparison of three low earth orbit satellite constellation systems to provide global broadband," Acta Astronaut, vol. 159, pp. 123-135, 2019/06/01/ 2019.
- [8] OneWeb. (2016). Application for Fixed Satellite Service by WorldVu Satellites Limited [SAT-

- LOI-20160428-00041] [Online]. Available: <https://fcc.report/IBFS/SAT-LOI-20160428-00041>.
- [9] Astrome Space Technologies SARL, "Astrome: SpaceNet Constellation Design Yellow Paper," 2019-06-23, 2019.
- [10] I. V. Karunanithi, C. J. M. Verhoeven, and E. W. McCune, "Solutions to Data Congestion in Space; mmWave Communication for Nano-Satellites," in 2019 IEEE Aerospace Conference, 2019, pp. 1-12.
- [11] K. S. Low, M. S. C. Tissera, and J. W. Chia, In-orbit Results of VELOX-II Nanosatellite (Proceedings of the 2016 IEEE Region 10 Conference). 2016, pp. 3658-3663.
- [12] A. T. Ltd, "Addvalue's Inter-Satellite Data Relay Terminal completes one year of in-orbit testing," ed, 2016.
- [13] A. Babuscia et al., "CommCube 1 and 2: A CubeSat Series of Missions to Enhance Communication Capabilities for CubeSat," in 2013 IEEE Aerospace Conference (IEEE Aerospace Conference Proceedings, 2013).
- [14] Z. QU, G. ZHANG, H. CAO, and A. J. XIE, "LEO Satellite Constellation for Internet of Things," IEEE Access, 2017.
- [15] M. D. Sanctis, E. Cianca, G. Araniti, I. Bisio, and R. Prasad, "Satellite Communications Supporting Internet of Remote Things," IEEE INTERNET OF THINGS JOURNAL, pp. VOL 3, NO. 1, FEBRUARY 2016.
- [16] Q. Yang, D. I. Laurenson, and a. J. A. Barria, "On the Use of LEO Satellite Constellation for Active Network Management in Power Distribution Networks," IEEE TRANSACTIONS ON SMART GRID, pp. VOL. 3, NO. 3, SEPTEMBER 2012.
- [17] M. Corici et al., "Assessing satellite-terrestrial integration opportunities in the 5G environment," September 2016.
- [18] L. Yushi, J. Fei, and Y. Hui, "Study on Application Modes of Military Internet of Things (MIOT)," 2012 IEEE International Conference on Computer Science and Automation Engineering (CSAE), 2012.
- [19] IoT Academy. (2019). IoT Connectiviteit LPWAN update 2019: Wat is er beschikbaar in Nederland en daarbuiten? [Online]. Available: <https://premium.nl/wp-content/uploads/2019/01/20190124-IoT-whitepaper-LPWAN.pdf>.
- [20] Lacuna Space. (2019). Lacuna Space Achieves Major Milestone for LoRa® in Space. [Online]. Available: <http://www.parabolicarc.com/2019/08/15/lacu>

- [na-space-achieves-major-milestone-for-lora-in-space.](#)
- [21] Sigfox. (2019). Sigfox Radio Configurations [Online]. Available: <https://build.sigfox.com/sigfox-radio-configurations-rc>.
- [22] Accent Systems. (2019). Differences between Nb-IoT and LTE-M. [Online]. Available: <https://accent-systems.com/blog/differences-nb-iot-lte-m/>.
- [23] Telesat Canada. (2016). Application for Fixed Satellite Service by Telesat Canada [SAT-PDR-20161115-00108] [Online]. Available: <https://fcc.report/IBFS/SAT-PDR-20161115-00108>.
- [24] Telesat Canada. (2017). Application for Fixed Satellite Service by Telesat Canada [SAT-PDR-20170301-00023] [Online]. Available: <https://fcc.report/IBFS/SAT-PDR-20170301-00023>.
- [25] Space Exploration Holdings. (2016). Application for Fixed Satellite Service by Space Exploration Holdings, LLC [SAT-LOA-20161115-00118] [Online]. Available: <https://fcc.report/IBFS/SAT-LOA-20161115-00118>.
- [26] Space Exploration Holdings. (2017). Application for Fixed Satellite Service by Space Exploration Holdings, LLC [SAT-LOA-20170301-00027] [Online]. Available: <https://fcc.report/IBFS/SAT-LOA-20170301-00027>.
- [27] Space Exploration Holdings. (2018). Application for Fixed Satellite Service by Space Exploration Holdings, LLC [SAT-MOD-20181108-00083] [Online]. Available: <https://fcc.report/IBFS/SAT-MOD-20181108-00083>.
- [28] Space Exploration Holdings. (2019). Application for Fixed Satellite Service by Space Exploration Holdings, LLC [SAT-MOD-20190830-00087] [Online]. Available: <https://fcc.report/IBFS/SAT-MOD-20190830-00087>.
- [29] OneWeb. (2017). Application for Fixed Satellite Service by WorldVu Satellites Limited [SAT-LOI-20170301-00031] [Online]. Available: <https://fcc.report/IBFS/SAT-LOI-20170301-00031>.
- [30] OneWeb. (2018). Application for Fixed Satellite Service by WorldVu Satellites Limited [SAT-MOD-20180319-00022] [Online]. Available: <https://fcc.report/IBFS/SAT-MOD-20180319-00022>.
- [31] SpaceNews_Inc. (2018). OneWeb scales back baseline constellation by 300 satellites - SpaceNews.com [Online]. Available: <https://spacenews.com/oneweb-scales-back-constellation-by-300-satellites/>.
- [32] Astrome Space Technologies SARM, "Astrome's SpaceNet: Ubiquitous Internet For Real," 2019-07-08 2019.
- [33] Audacy Corporation. (2016). Application for Fixed Satellite Service Other by Audacy Corporation [SAT-LOA-20161115-00117] [Online]. Available: <https://fcc.report/IBFS/SAT-LOA-20161115-00117>.
- [34] D. C. BESTE and M. IEEE, "Design of Satellite Constellation for Optimal Continuous Coverage," IEEE TRANSACTIONS ON AEROSPACE AND ELECTRONIC SYSTEMS, pp. AES-14, NO. 3, MAY 1978.
- [35] Goyal et al., "poliastro/poliastro: poliastro 0.13.0 (late PyAstro '19 edition)," 2019.
- [36] P. a. V. Ramachandran, G., "Mayavi: 3D Visualization of Scientific Data," Computing in Science & Engineering, vol. 13, 2, pp. 40--51, 2011.
- [37] F. L. Markley, "Kepler Equation solver," Celestial Mechanics & Dynamical Astronomy, journal article vol. 63, no. 1, pp. 101-111, March 01 1995.
- [38] M. Handley, "Delay is Not an Option," presented at the Proceedings of the 17th ACM Workshop on Hot Topics in Networks - HotNets '18, 2018. [Online]. Available: http://delivery.acm.org/10.1145/3290000/3286075/p85-Handley.pdf?ip=145.94.9.203&id=3286075&acc=ACTIVE%20SERVICE&key=0C390721DC3021FF%2E512956D6C5F075DE%2E4D4702B0C3E38B35%2E4D4702B0C3E38B35&acm_=1563434987_db0a1051c1be0136bb125fc6564e008a.
- [39] Telesat Canada. (2019). World's First 5G Backhaul Demo over LEO Satellite | Telesat [Online]. Available: <https://www.telesat.com/news-events/worlds-first-5g-backhaul-demo-over-leo-satellite>.
- [40] OneWeb. (2019). OneWeb's Satellites Deliver Real-Time HD Streaming from Space | OneWeb [Online]. Available: <https://www.oneweb.world/media-center/onewebs-satellites-deliver-real-time-hd-streaming-from-space>.